



DIGITAL ACCESS TO SCHOLARSHIP AT HARVARD

OddEven Effects in Charge Transport across Self-Assembled Monolayers

The Harvard community has made this article openly available.
[Please share](#) how this access benefits you. Your story matters.

Citation	Thuo, Martin M., William F. Reus, Christian A. Nijhuis, Jabulani R. Barber, Choongik Kim, Michael D. Schulz, and George M. Whitesides. 2011. "OddEven Effects in Charge Transport Across Self-Assembled Monolayers." <i>Journal of the American Chemical Society</i> 133, no. 9: 2962–2975.
Published Version	doi:10.1021/ja1090436
Accessed	February 16, 2015 7:50:15 PM EST
Citable Link	http://nrs.harvard.edu/urn-3:HUL.InstRepos:12967807
Terms of Use	This article was downloaded from Harvard University's DASH repository, and is made available under the terms and conditions applicable to Open Access Policy Articles, as set forth at http://nrs.harvard.edu/urn-3:HUL.InstRepos:dash.current.terms-of-use#OAP

(Article begins on next page)

Odd-Even Effects in Charge Transport Across Self-Assembled Monolayers.

*Thuo, Martin M.; Reus, William F.; Nijhuis, Christian A.; Barber, Jabulani R.; Kim, Choongik; Schulz, Michael D.; and Whitesides, George M.**

Department of Chemistry and Chemical Biology, Harvard University, 12 Oxford St,
Cambridge, MA 02138, USA

Corresponding author:

Tel.: 617 458 9430

Fax.: 617 458 9857

e-mail: gwhitesides@gmwgroup.harvard.edu

Abstract

This paper compares charge transport across self-assembled monolayers (SAMs) of *n*-alkanethiol containing odd and even numbers of methylenes. Ultraflat template-stripped silver (Ag^{TS}) surfaces supported the SAMs, while top-electrodes of eutectic gallium-indium (EGaIn) contacted the SAMs to form metal/SAM//oxide/EGaIn junctions. The EGaIn spontaneously reacts with ambient oxygen to form a thin (~ 2 nm) oxide layer. This oxide layer enabled EGaIn to maintain a stable, conical shape (convenient for forming microcontacts to SAMs) while retaining the ability to deform and flow upon contacting a hard surface. Conical electrodes of EGaIn conform (at least partially) to

SAMs, and generate high yields of working junctions. Ga₂O₃/EGaIn top electrodes enable the collection of statistically significant numbers of data in convenient periods of time. The observed difference in charge transport between *n*-alkanethiols with odd- and even- numbers of methylenes – the “odd-even effect” – is statistically discernable using these junctions, and demonstrates that this technique is sensitive to small differences in the structure and properties of the SAM. Alkanethiols with an even number of methylenes exhibit the expected exponential decrease in current density (*J*) with increasing chain length, as do alkanethiols with an odd number of methylenes. This trend disappears, however, when the two datasets are analyzed together; alkanethiols with an even number of methylenes typically show higher *J* than homologous alkanethiols with an odd number of methylenes. The precision of the present measurements, and the statistical power of the present analysis, were only sufficient to identify, with statistical confidence, the difference between an odd and even number of methylenes with respect to *J*, but not with respect to the tunneling decay constant, β , or the pre-exponential factor, J_0 .

Introduction

This paper describes charge transport through tunneling junctions of self-assembled monolayers (SAMs) of *n*-alkanethiols, formed on ultra-flat Ag electrodes, contacted with a liquid top-electrode. It compares charge transport through SAMs of *n*-alkanethiols having odd and even numbers of methylene groups ($\text{SC}_{n-1}\text{CH}_3$ where $n = 9 - 18$), and demonstrates, using statistical analysis, the existence of an “odd-even effect”. This work constitutes a benchmark both for the theory of charge tunneling in thin organic films, and for future experimental work with these systems.

We used EGaIn (a liquid eutectic alloy, 75.5 wt % Ga and 24.5 wt % In) as a liquid-metal top-electrode, and measured current density, J (A/cm^2), through SAMs as a function of applied bias, V . Under ambient conditions, EGaIn has a thin (~ 2 nm) surface layer composed predominantly of gallium(III) oxide (Ga_2O_3).¹ This composite structure — bulk liquid metal supporting a thin rigid, superficial oxide — constitutes a semi-conformal (i.e. conformal on length-scales exceeding $1 \mu\text{m}$, but probably not conformal on the nanoscale) electrode. Together with ultra-flat, template-stripped Ag substrates and alkanethiol SAMs, this top-electrode is a crucial component of a system that makes it practical to generate large numbers of $J(V)$ data (~ 500 measurements in one day), and gives high yields ($\sim 80\%$) of non-shortening junctions; this combination enables meaningful statistical analysis, and opens the door to systematic physical-organic studies of charge transport across organic thin films.

Across the range of molecular lengths, d , examined, we found that, for a given applied voltage, J (as expected) obeys a simple approximation (Equation 1) of the Simmons equation;

$$J = J_0 e^{-\beta d} \quad (1)$$

where β (n_C^{-1}) is the tunneling decay constant, d (in n_C) is the thickness of the SAM, and J_0 is the current density across a hypothetical SAM lacking an alkyl chain (i.e. $d = 0$).

The magnitude of J_0 is determined by the interfaces between the electrodes and the SAM.

SAMs of odd-numbered n -alkanethiols differ from corresponding SAMs of even-numbered n -alkanethiols with respect to many properties, including structure, surface free energy, kinetics of molecular exchange, tribology, kinetics of electron transfer, electrochemistry, reactivity, and packing density.²⁻⁴ In addition to SAMs, liquid crystals and molecule-capped quantum dots also exhibit odd-even effects.^{2,5-38} With respect to charge transport in organic systems, the effects of odd- or even- numbered n -alkyl or oligomethylene groups have been observed in pentacene-based field-effect transistors,³⁹ H-bonded assemblies,⁴⁰ and biphenyl-based systems.⁴¹ It is, thus, not astonishing, although still noteworthy, that odd-even effects also influence charge transport across SAMs of alkanethiols.^{2,34-38,42,43}

We synthesized a series of n -alkanethiols with an odd number of carbons (SC_n where $n = 9, 13, 17$). Commercially available undecanethiol, pentadecanethiol, and all even- methylene-containing thiols, were purified before use (see supporting information). We formed SAMs on template-stripped silver (abbreviated Ag^{TS}) (Figure 1). We then fabricated molecular tunnel junctions by bringing the SAMs into contact with a $Ga_2O_3/EGaIn$ liquid top-electrode (We use this nomenclature to emphasize the importance of the surface film of Ga(III) oxide, but note that this description is a simplification of a more complex surface.⁴⁴

Using statistical tools, we showed, with greater than 95% confidence, that the results from SAMs with even and odd numbers of methylenes belong to separate datasets (i.e. analyzing the two series separately led to more consistent interpretations of the results, according to the simplified Simmon's model, than did analyzing them together); thus, we concluded that there is an odd-even effect. While the data from SAMs with even and odd numbers of methylenes demanded separate fits to eq. **1**, our statistical analysis was not sufficiently powerful to distinguish between the values of J_0 and β for these two series.

Four characteristics of these junctions enabled us to perform physical-organic experiments relating molecular structure to charge transport: i) a semi-conformal top-electrode, ii) ultra-flat (root-mean-square roughness < 0.5 nm as measured by atomic force microscopy) template-stripped silver substrates, iii) carefully purified thiols, and iv) the ability to conduct measurements under ambient conditions (i.e. without a clean room, a polymer interface, or a solvent bath). The first three characteristics of these junctions reduced the density of defects leading to shorts and outliers (defined below) and increased the yield of working junctions. The fourth characteristic allowed the collection of large numbers of data within a convenient timeframe (~ 500 $J(V)$ traces in 8 hours) and, thus, enabled robust statistical analysis.

Figure 1. Schematic description of the preparation of the template-stripped silver, Ag^{TS}, substrates. i). On a clean Si(111) wafer, having a native SiO₂ surface layer, we deposited a 450 - nm thick Ag film by e-beam evaporation. ii and iii). Glass supports were mounted on the thin film using photo-curable optical adhesive. A variety of sizes can be used as support and there is no need for size specification. iv). After photo-curing the optical adhesive, the metal film around the glass support was cut out using a razor blade. v). the silver film, with its supporting glass, was lifted off to expose an ultra-flat Ag film. The detached Ag^{TS} surface was then immediately (~30 sec) used to prepare SAMs by transferring (through air) into a solution of alkanethiol. The supporting information gives more details on this procedure.

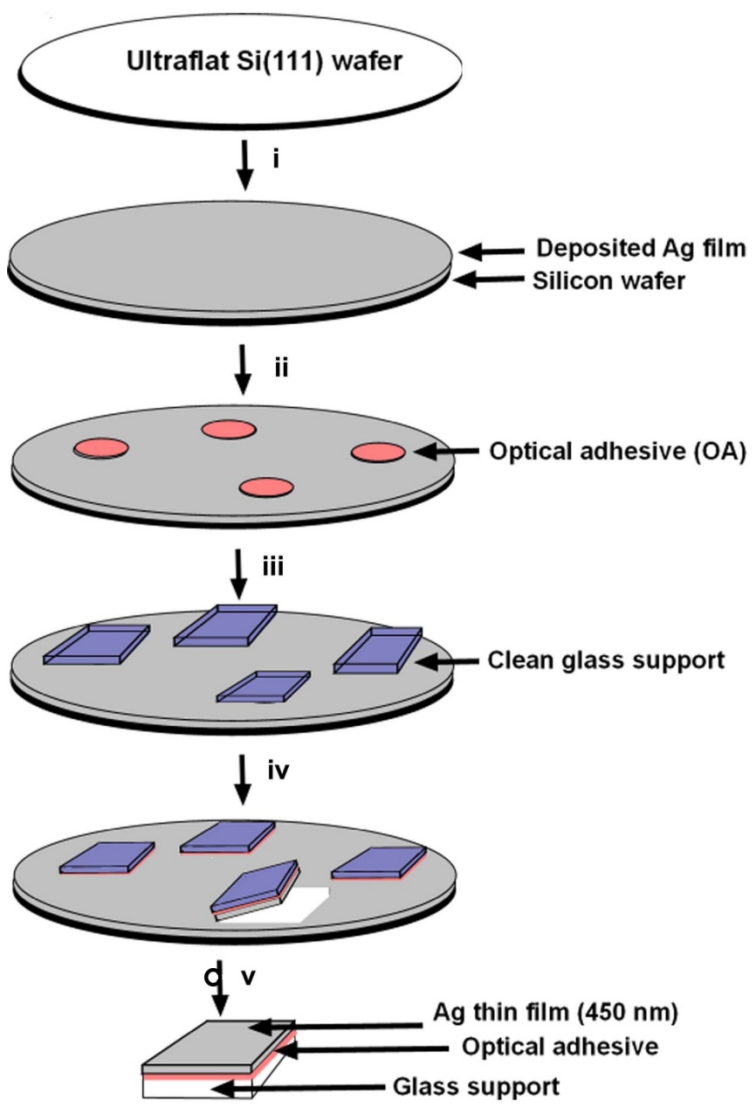


Fig 1.

Figure 2. a) A schematic illustration of the apparatus used to make measurements of tunnel currents across SAMs. b) A picture of a working $\text{Ag}^{\text{TS}}/\text{SAM}/\text{Ga}_2\text{O}_3/\text{EGaIn}$ junction. The junction was fabricated by gently lowering the EGaIn tip onto a substrate bearing the SAM, and contact was confirmed by the convergence of the tip with its reflected image on the substrate surface to give a closed electrical circuit. The connection was also confirmed by passing current through the closed circuit. c). An illustration of the anatomy of a perfect junction showing the van der Waals interface between the SAM and the EGaIn/oxide top-electrode and how the deformable liquid metal conforms to features on the surface.

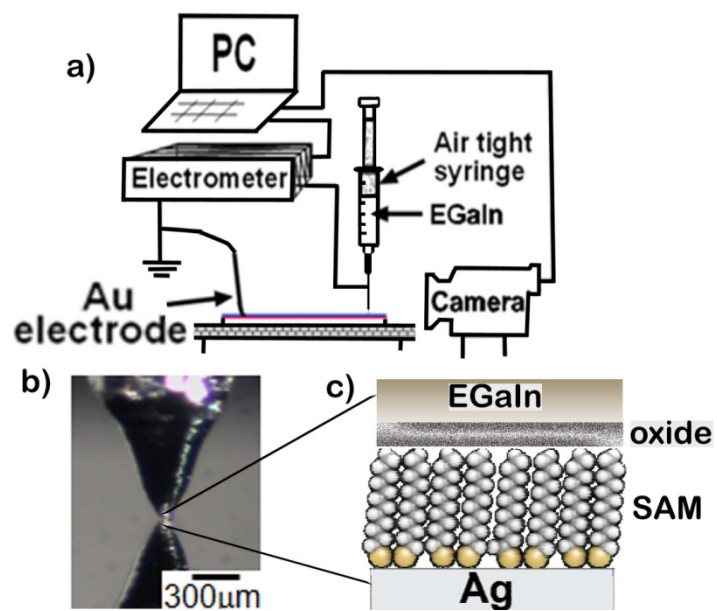


Fig. 2

Charge transport through insulating organic matter almost certainly occurs (at least over distances of less than a few nanometers) *via* non-resonant coherent tunneling.^{39,45-55} Understanding the relationship between molecular structure and electronic properties in organic systems would improve our ability i) to model electron transport in relevant biological systems (e.g. redox proteins) and ii) to evaluate the potential of, and perhaps to design, electronic devices based on organic components. To these ends, we wished to develop a convenient and reliable technique for conducting physical-organic experiments designed to probe the fundamental principles of charge-transport across thin (< 3 nm) films of structurally well-defined organic matter.

Systematic studies of charge transport in small molecules have been experimentally difficult, and there is currently no convenient, broadly accepted platform with which to perform such studies. Probing the difference between SAMs of *n*-alkanethiols with odd and even numbers of methylene units is an example of a systematic, physical-organic study designed to give information about the effect of the non-covalent interface (see below) between the SAM and an electrode on charge transport.

We, and others,^{50,56-68} have begun an effort to develop and prove reliable protocols for measuring charge transport across SAMs. Our approach features a semi-conformal (mechanically compliant on the micron-scale but probably not conformal on smaller scales) liquid top-electrode, EGaIn (a liquid eutectic alloy of gallium and indium), whose surface is largely, or entirely, covered with a thin oxide film (predominantly gallium oxide).⁴⁴ We believe that this oxide film is crucial to generating

high yields of working junctions (see below) and, thus, enables the collection and statistical analysis of large numbers of data.

There are, however, several features of the layer of Ga₂O₃ that merit careful consideration and discussion. The electrical resistivity ($\sim 10^6 \Omega\text{-cm}$)¹ of this oxide layer is at least three orders of magnitude smaller than that of a SAM of SC₉ (the most conductive SAM we are able to measure reliably). Since the thickness of this layer ($\sim 2 \text{ nm}$) is approximately equal to that of a typical SAM, the resistance of this layer is several orders of magnitude less than that of a SAM. The roughness of the layer of Ga₂O₃ probably causes the electrode to be non-conformal over distances up to $1 \mu\text{m}$, a characteristic that adds uncertainty to the estimation of the area of junctions. Based on experiments and simulations that will be discussed elsewhere,¹ however, we believe that overestimation of junction area introduces a systematic error, as opposed to a random error. In other words, distributions of J may be shifted, but not broadened, by this error. Furthermore, we have no reason to suspect that this error varies with the length of the SAM; therefore, it should not affect comparisons across alkanethiols of different lengths. Finally, the surface of the Ga₂O₃ may be contaminated with a complete or partial layer of adsorbed organics. The effect of this layer on charge transport is unknown. We show in this work that, despite these cautionary features, the Ga₂O₃/EGaIn electrode yields results that are reproducible and consistent with a wide range of prior work on charge transport through SAMs of *n*-alkanethiols. Further, the distributions observed for compounds at the extremes of the series (SC₉ and SC₁₀ on the lower end and SC₁₆ – SC₁₈ on the upper end) were consistently narrower than those of compounds in the middle of the series (SC₁₁ – SC₁₅,

with the exception of SC₁₃, see below). We infer that the nature of the interfaces in the junctions does not dominate the broad distributions observed in the middle of the series.

Background

Some common features have emerged in many of the systems for studying charge transport in organic matter. Self-assembled monolayers (SAMs) are an obvious candidate for the organic component of such systems, since SAMs are readily prepared using organic precursors having a wide range of structures. Gold and silver are currently the most widely used metal substrates for forming SAMs. Gold has the advantage of being impervious to oxidation under ambient conditions; however, the alkyl chains of SAMs of alkanethiols on gold are tilted at an angle of $\sim 30^\circ$ to the surface normal, compared to $\sim 10^\circ$ on Ag.⁶⁹⁻⁷² Outka *et. al.*⁷³ and Ulman *et. al.*⁷⁴ illustrated that an optimal packing density of *n*-alkanethiols on a metal surface depend on a combination of the tilt angle and lattice spacing. Subsequently it has been shown that thiolate SAMs on Ag(111) have 26% more chains/unit area than on Au(111).^{75,76} While most studies use substrates (whether Au or Ag) as-deposited by electron-beam evaporation, we have previously shown that template-stripping leads to flatter surfaces (rms roughness; Ag^{TS} = 1.2 vs 5.1 for as deposited, and Au^{TS} = 0.6 vs 4.5 for as deposited)⁷⁷ and increases the yield of non-shortening junctions when using a Hg top-electrode.^{77,78}

While there is a broad consensus on the use of SAMs and, to a large extent, Au or Ag substrates, myriad strategies exist for forming a second (top) contact to the SAM. Historically, forming an electrical contact with a SAM has been challenging. Lee *et al* have shown that direct evaporation of metallic top-electrodes onto SAMs damages the

monolayer,^{56,59,79,80} and results in low yields (< 5%) of non-shortening junctions, and in the formation of metal filaments due to the migration of metal atoms through defect sites in the SAM. With the notable exception of Lee *et al.*^{56,59,60} who reported yields, and statistically defined ‘working devices’ for these junctions, studies of evaporated metal top-electrodes have not included adequate statistical analysis of $J(V)$ data, and are, thus, unable to discriminate between molecular effects and artifacts. When performed carefully, these studies can afford reproducible results, but only when sufficiently large numbers of electrodes are generated to define the system statistically. These types of preparations and measurements are too arduous for physical-organic studies. Furthermore, many of these studies use SAMs formed from structurally complex molecules, without adequate characterization of the probably complex and often disordered structure of these SAMs.

Other strategies for measuring charge transport across SAMs fall into two arbitrary categories: i) small-area (< 1 μm^2 , or 1 – 10⁶ molecules) measurements, which can generate high-quality data but are time-consuming to perform and require specialized techniques and instruments, and ii) large-area (> 100 μm^2 , or 10⁸ – 10¹² molecules) measurements aimed at conveniently generating sufficiently large numbers of data to allow statistical assessment of experimental uncertainty. In the first category, Lindsay and co-workers,^{50,81-83} Frisbee and co-workers, Lee and co-workers,^{56,58,84-86} Venkataraman and co-workers,⁸⁷⁻⁸⁹ and others⁹⁰ have employed conducting probe tips (STM, cpAFM) to measure charge transport across SAMs. Break junctions, both mechanically controllable and electromigration-based, are another form of small-area junctions (consisting of one to several molecules trapped between two electrodes^{60,91-94}).

Break junctions have the distinct advantage of incorporating a gate electrode, although they are tedious to prepare. Kushmerick *et al.* developed a technique for measuring small area molecular junctions ($\sim 10^3$ molecules) through a crossed-wire tunneling junction.^{95,96} Two gold wires (10 μm diameter) are crossed, with one parallel and the other perpendicular to an external magnetic field. A current flowing through the perpendicular wire engenders a Lorenz force that controls the spacing between the two wires. In this technique one wire – coated with a π -conjugated self-assembled monolayer – creates a metal-molecule-metal junction.⁹⁷

For large-area measurements of SAMs on Ag, we and others have employed a hanging drop of Hg, on which a second SAM has been formed.^{53,78,98-105} Recently, Akkerman *et al.* fabricated large numbers of molecular junctions in parallel using a spin-cast, conductive polymer film (PEDOT:PSS) on top of the SAM to make electrical contacts, and to protect the organic molecules from damage due to exposure of evaporated metal atoms.^{62-67,106} The conductive polymer film may be protective and provide a good contact; unfortunately, it also introduces unresolved ambiguities in the system and seems to produce measurements that are rather different from other methods ($\beta_{\text{even}} = 0.66 \pm 0.04$ per carbon, where consensus value from other methods is $\beta_{\text{even}} = \sim 1$ per carbon, n_{C}^{-1} , for n -alkanethiol SAMs).⁶³

Although a wide range of methods have been employed to measure charge transport across SAMs, all *successful* techniques share the characteristic that they have a non-metallic layer between the SAM and the top electrode: a thin film of insulating metal oxide, a small gap of air or vacuum between a probe tip and the SAM, a second SAM on Hg, or a layer of conductive polymer between the SAM and an evaporated Au electrode.

The most probable function of this “protective layer” in these junctions is to prevent metal atoms from migrating through defect sites under electrostatic pressure and causing filaments to form and thus to cause shorts and other artifacts. In our current work, a ~ 2-nm thick self-passivating semiconducting oxide (predominantly Ga₂O₃) layer performs this function (see above and supporting information).¹

The best characterized types of SAM, both structurally and with respect to charge transport, are those formed by *n*-alkanethiols on Au and Ag.^{3,52,70,94,107-127} The mechanism of charge transport through SAMs is believed to be hole tunneling, with the height of the tunneling barrier defined by the large HOMO-LUMO gap (8-10 eV) of the alkanethiols forming the SAM.¹²⁸ The barrier width is defined by the thickness of the SAM (~1-3 nm). The value of the tunneling decay constant, β , (Equation 1) reported in the literature for the commercially available even-numbered alkanethiols (CH₃(CH₂)_{*n*-1}SH where *n* = 10, 12, 14, 16, 18), ranges from 0.51 to 1.13 *n*_C⁻¹ with a majority of the value in the range 0.75 – 1.1 *n*_C⁻¹.^{59,63,65,129} Akkerman and others^{39,53,128,130} attempted to distinguish charge transport across SAMs comprising odd- and even-number of methylenes experimentally, but did not succeed.

SAMs of *n*-alkanethiols assembled on metal surfaces via a covalent interaction pack with a distinct tilt that is characteristic of the substrate (e.g. ~10° for Ag, ~30° for Au, with respect to the surface normal). The hybridization, and hence both the geometry and stereo-electronic environment, around the sulfur atom is also believed to depend on the substrate (sp³ for Au and sp for Ag).^{3,70,131} For *n*-alkanethiols in an all-*trans* extended conformation, three parameters combine to determine the orientation of the terminal group at the surface of the SAM: i) the tilt angle, ii) the hybridization around the sulfur

atom, and iii) the number of methylenes in the alkyl chain. The orientation of the terminal methyl group, in turn, affects the surface properties of the SAM, and therefore dictates the nature of interactions with other materials.

In reality, SAMs are not extended, perfect, 2D crystals, but have many defects: pin-holes, domain boundaries, disordered regions, impurities physisorbed on or incorporated into the SAM, and defects due to vacancy islands, step edges, and grain boundaries in the substrate, to name a few.^{3,70,78,132} These defects cause many of the molecules in a SAM to adopt conformations other than the ideal all-*trans* extended conformation. Defects in the SAMs may thus blur the distinction between the surfaces presented by odd- and even-numbered alkanethiols – a distinction that would probably manifest itself most significantly in the difference in the orientations of their terminal methyl groups in the *trans*-extended conformation. The more disordered the SAM, the less important we expect intrinsic, conformational-based differences between odd- and even- *n*-alkanethiols to be.

Liquid top-electrodes (e.g. Hg, Hg-SR and Ga₂O₃/EGaIn), form reproducible contacts with SAMs and, can be used to generate large numbers of data, whose distributions can be analyzed statistically. Although they have their own limitations, liquid top-electrodes are much easier to use, and require less specialized equipment, than other methods (e.g. AFM tip-based techniques, or break junctions). This paper extends previous work on the Ga₂O₃/EGaIn- based system of measuring tunneling currents across SAMs on Ag^{TS}, and demonstrates an odd-even effect in charge transport across alkanethiol SAMs.

Our initial estimate, using a Ga₂O₃/EGaIn top electrode, was of $\beta_{\text{even}} \sim 0.54 n_C^{-1}$.¹³³ This value lies well outside the band of values more commonly reported in the literature (0.75 – 1.1 n_C^{-1}). We now believe this number to be incorrect, and to reflect our inappropriate selection of data from a sparse and (at that time) noisy dataset. We measured the value of J (A/cm²) for four chain lengths (SC₁₀, SC₁₂, SC₁₄ and SC₁₆) but used only three (SC₁₂, SC₁₄ and SC₁₆) in determining the value of β_{even} . The collected results should, however, have been analyzed without excluding any data. We made three errors: i) for reasons that seemed valid at the time, but, in retrospect were, not, we discarded the data for SC₁₀. Had we instead fitted the data derived from all four alkanethiols, we would have estimated β close to 1.0 n_C^{-1} , (albeit with a large experimental uncertainty). ii) In these early stages of development of the Ga₂O₃/EGaIn electrode, we did not appreciate a number of experimental variables, and the collected data were much more scattered than the data in this paper. The quantity of data, both in the number of alkanethiols used and in the number of $J(V)$ traces collected, was insufficient for a reliable statistical analysis. iii) The purity of the n-alkanethiols was not carefully controlled or monitored throughout the study.

In this study, we have corrected these errors by; i) including *all* data from our analysis (we exclude *no* data), ii) collecting more data, both in numbers of alkanethiols molecules used (five per series, for a total of ten, as opposed to four in the previous work) and in numbers of $J(V)$ traces measured (an increase of a factor of three to ten over our previous work¹³³), and iii) purifying all compounds before use. The result is a tunneling decay constant ($\beta_{\text{even}} = 1.12 n_C^{-1}$) for even-numbered alkanethiols that agrees well with the consensus of results based on other liquid metal electrodes.^{78,134} In this work, we also

obtained $\beta_{\text{odd}} = 1.03 \text{ nC}^{-1}$ for odd-numbered alkanethiols. Although numerically different from the value obtained from the even series, the difference between β_{even} and β_{odd} is *not* statistically significant, according to a two-tailed Student's t-test ($p > 0.1$). The lack of a statistically significant difference is not, however, a statement that the values of β_{odd} and β_{even} are the same, and this apparent difference suggests a direction for further investigation. Fitting the two series yields values of J_0 with overlapping ranges of uncertainty.

Experimental Design

Template-stripped Ag substrates. We used silver surface because the SAMs have a smaller tilt angle ($\sim 10^\circ$ to the surface normal) which leads to better packing (SAMs on Ag(111) surfaces have $\sim 26\%$ more alkyl chains/unit area than do those on Au(111)^{75,76}). We use template-stripped silver (Ag^{TS}) substrates because the surface is flatter, and probably cleaner, than the exposed, top surface of electron-beam evaporated ("as deposited") films (Ag^{AD}).⁷⁷ We previously found that the use of template-stripped substrates rather than as-deposited substrates significantly increased the yield of working junctions in SAM-based devices.^{77,78}

Liquid metal top electrode. EGaIn is commercially available in high purity, easy to handle, and non-toxic. On exposure to ambient conditions, EGaIn forms a thin ($\sim 2 \text{ nm}$) self-limiting passivating gallium(III) oxide film on the surface.^{44,135} The remarkable mechanical strength of this film is responsible for the ability of EGaIn to adopt and maintain non-equilibrium shapes (e.g. the cone used to make electrical contacts in this paper).¹³³

Self-assembled monolayers. Self-assembled monolayers of n-alkanethiols on silver give well-defined organic structures. These SAMs provide an obvious substrate for studying charge transport because they i) are constrained in one dimension to the length of the molecule (~2 nm), yet ii) can be arbitrarily large in the other two dimensions, and iii) can be readily modified, *via* simple organic reactions, to increase the complexity of the molecules being investigated.

Choice of *n*-alkanethiols. We used compounds of intermediate chain lengths, $9 \leq n \leq 18$. This range avoided problems associated with long chains (low solubility in polar solvents and current densities too low to be measured with our electrometer) and the empirical difficulties (e.g. shorts and noisy, unstable junctions) associated with short chains. The alkanethiols used (SC₉-SC₁₈) are approximately 1.0 – 2.5 nm long. This choice of chain lengths also allowed comparison with information in the literature, because SAMs of alkanethiols in this range of chain lengths have been widely studied by others.

Purity of thiols. we emphasize the importance of using highly pure (> 99%) alkanethiols. As previously observed by us and others, impurities in the thiols can lead to defects in the SAM and, therefore, to artifacts and decreased yields of working junctions.

Log-Normal Distributions of *J*. As noted in the Results and Discussion section, we observed log-normal distributions of *J* (i.e. $\log(|J|/[A/cm^2])$, written as $\log(|J|)$ for convenience, was normally distributed). Log-normal distributions of current have been observed previously in molecular junctions by us (using Hg-drop junctions)⁷⁸ and others (using polymer buffer layers,^{63,106,130} nanopores,^{60,136,137} and cpAFM¹³⁸⁻¹⁴⁰). In all of these studies, the explanation for the apparent normal distribution of $\log(|J|)$ is that *J*

depends exponentially on a physical parameter that is normally distributed, such as the thickness of the tunneling barrier between two electrodes. This dependence on thickness, across all the above techniques, leads to a range of J that span several (3 – 8) orders of magnitude. We believe that defects in the Ag^{Ts} substrate, the SAM, and the Ga₂O₃/EGaIn top electrode lead to variations in the local separation between electrodes, d (eq. 1).

These variations, are presumably, normally distributed, and thus give rise to log-normal distributions of J (appearing as Gaussian peaks in histograms of $\log|J|$).

Analyzing Distributions of $\log(|J|)$ vs. J . Since many of the tools of statistical analysis assume that the data being analyzed are normally distributed, directly analyzing distributions of J is difficult. A more statistically tractable approach than directly handling J is to work with $\log(|J|)$ (since distributions of the latter are normal) and subsequently to map the results of the analysis of $\log(|J|)$ onto the domain of J . For instance, we wish to determine the population mean, μ_J , and standard deviation, σ_J , of J . Calculating the arithmetic average of J ($\langle J \rangle = (\sum_i J_i)/N_J$, where $\sum_i J_i$ is the sum of all measured values of J , and N_J is the number of measured value of J) yields an estimate of the population mean, μ_J , strongly biased toward high values of J . Similarly, the straightforward calculation of the arithmetic standard deviation of J ($s = [(\langle (J - \langle J \rangle)^2 \rangle)]^{1/2}$) also yields a biased value. On the other hand, since $\log(|J|)$ is normally distributed, familiar methods can be used to estimate the population mean, μ_{\log} , and standard deviation, σ_{\log} , of $\log(|J|)$ (μ_J is related to μ_{\log} by the equation $\log(\mu_J) = \mu_{\log}$, and σ_J to σ_{\log} by $\log(\sigma_J) = \sigma_{\log}$). Reporting error is also easier for $\log(|J|)$ than for J . For instance, we can correctly report the error on an estimate of the population mean of $\log(|J|)$ as

$\mu_{\log} \pm \sigma_{\log}$. The expression $\mu_J \pm \sigma_J$ does not make sense as a description of the error in the estimate of the population mean of J , if the distribution of J is normal in $\log(|J|)$.

Results and Discussion

Synthesis and Purification of n-Alkanethiols. We synthesized the SC₉, SC₁₃, SC₁₇, and SC₁₉ alkanethiols from their corresponding primary alkylbromides. The alkylbromides were converted to isothiuronium salts followed by treatment with NaOH, which gave the desired thiol. The products, after chromatographic purification, were characterized by NMR and spectral data compared to literature.

We established, and emphasize, the importance of purity of the thiols on the reproducibility of the subsequent electrical measurements. We ensured that the alkanethiols had purity of >99% by ¹H NMR before use. The n-alkanethiols degrade over time, especially at elevated temperature and in the presence of oxygen, by forming either disulfides or sulfur oxides (see example in Figure S7a; 2.67 ppm and 3.73 ppm respectively). To ensure that our thiols were pure, we either recrystallized them under an inert atmosphere using cannula-transfer techniques, or purified them by flash column chromatography, immediately before storage and where necessary before use. The supporting information gives a detailed description of our procedures. We found that a single re-crystallization often did not give sufficiently pure thiols for our uses, especially when the starting reagents were partially oxidized.

Preparation and Measurement of Junctions. We prepared the ultra-flat template stripped surfaces, Ag^{TS}, by depositing 450 nm of Ag metal onto a clean Si(111)

wafer using an electron-beam evaporator, then detaching (stripping) the Ag film from the Si wafer using a glass support as previously described and illustrated in Figure 1.¹³² SAMs were generated by immersing the Ag^{TS} in a degassed solution of a thiol for 3 h (see supporting information for detailed procedures). The Ag^{TS}/SAM//Ga₂O₃/EGaIn junctions were fabricated as previously discussed.^{132,133} The reflection of the tip image on the silver surface was used to confirm a contact between a SAM and the EGaIn top-electrode during junction fabrication (see supporting info).

We collected 380 – 2800 J/V traces for every n-alkanethiol (synthesized or commercially available) using Ag^{TS}/SC_nSAM//Ga₂O₃/EGaIn junctions. For each alkanethiol synthesized, a minimum of 11 junctions (Ag^{TS}-SC_n//Ga₂O₃/EGaIn) were fabricated with a maximum of 11 junctions fabricated per Ag^{TS} chip (a Ag^{TS} surface on a glass substrate). Except in the case of SC₉, we measured a minimum of two Ag^{TS} chips per molecule. On each junction a maximum of 21 $J(V)$ traces (one trace = 0V → +0.5V → -0.5V → 0V at steps of 50 mV with a 0.2 s delay) were recorded (Table 1).

Attempts to Measure n-Alkanethiols Longer than SC₁₈ and Shorter than SC₉ Failed. SAMs derived from n-alkanethiols longer than SC₁₈ yielded noisy and inconsistent $J(V)$ traces similar in shape and magnitude to an open circuit (i.e. a $J(V)$ trace measured with the Ga₂O₃/EGaIn electrode suspended in air. Based on a linear fit of our data (figure 5), we extrapolate a current density for SC₁₉ of 8.3×10^{-8} A/cm² at -0.5 V. For a typical junction, with an area of $\sim 500 \mu\text{m}^2$, the tunneling current at -0.5 V would be 4.2×10^{-13} A, which is below the detection limit ($\sim 10^{-12}$ A) of our electrometer. We attempted to measure current densities across SC₁₉ on different days and using different

substrates, but the data were highly inconsistent, and the $J(V)$ data had a very broad distribution ($\sigma_{\log} = 0.25 - 1.12$). Attempts to measure the $J(V)$ characteristics of SC₈ and SC₇ yielded similarly incoherent results. These measurements should not suffer from any limitations imposed by our electrometer; however, SAMs of n-alkanethiols shorter than SC₉, being liquid-like and loosely packed, may suffer from a large density of defects that cause large variations in J . We are exploring ways to improve and characterize SAMs of these short n-alkanethiols.

Statistically Analyzing Distributions of $\log(|J|)$. Charge-transport measurements of n-alkanethiols from SC₉ to SC₁₈ yielded values of J that were log-normally distributed (Figure 3); that is, the distributions of $\log(|J|/[A/cm^2])$ (hereafter written as $\log(|J|)$ for convenience) approximately fit Gaussian functions, whereas the distributions of J on a linear scale did not. The shape and width (related to σ_{\log}) of the distributions does not differ appreciably over the range of applied bias, from -0.5 V to 0.5 V (Figure 4). We describe all further analysis using data for $V = -0.5V$, but we are confident that the trends identified in this analysis are valid for other biases in the range measured.

In the Experimental Design section, we make the case for analyzing distributions of $\log(|J|)$, as opposed to J . That section introduces the population mean (μ_{\log}) and standard deviation (σ_{\log}) of $\log(|J|)$ and explains how these parameters relate to the distribution of J . Since knowing the shape of the distributions of J and $\log(|J|)$ is vital to performing a correct analysis, we emphasize the importance of collecting enough data to resolve this shape adequately. With the exception of SC₉, we collected at least 700 data points on at least 20 junctions for every compound (Table 1).

For an ideal normal distribution of $\log(|J|)$, μ_{\log} and σ_{\log} would be trivial to determine; however, our distributions are not ideal and suffer from shorts, outliers, and noise. We define a short as any junction yielding $\log(|J|) > 2$ (i.e. $J > 10^2$ A/cm²; this is approximately four orders of magnitude higher than the highest average J we measured through our most conductive SAM, SC₁₀). We do not quantitatively define outliers and noise, but we qualitatively identify the former, as values of $\log(|J|)$ in the histogram that fall well outside of the peak of the Gaussian function, and the latter, as values of $\log(|J|)$ that cause the shape of the peak to deviate from that of an ideal Gaussian function. For example, we would refer to the counts in the histogram of SC₁₀ (figure 3) between $\log(|J|) = -4.5$ and -2.5 as outliers, while we would designate the histogram of SC₁₄ a “noisy” histogram. The distinction between outliers and noise, however, has no bearing on our analysis.

There are two approaches to estimating μ_{\log} and σ_{\log} for a non-ideal distribution: i) taking the arithmetic mean and standard deviation of $\log(|J|)$ and ii) fitting a Gaussian function to the histogram of $\log(|J|)$ and extracting the fitting parameters (the mean and standard deviation of the Gaussian). The former approach has the advantage of yielding values of μ_{\log} and σ_{\log} that are insensitive to noise, although they are sensitive to shorts and outliers. The latter approach is essentially impervious to shorts and outliers, but may be greatly affected by noise. As is evident in Table 2, the estimates of μ_{\log} and σ_{\log} obtained using these two approaches can differ by as much as half an order of magnitude. Since the distinction between noise and outliers hinges on the parameters of the Gaussian fit, evaluating which approach to use can be difficult. Because of the dramatic influence of shorts on the arithmetic mean and standard deviation of $\log(|J|)$, however, we elected

to work with values of μ_{\log} and σ_{\log} determined using the Gaussian fit. Figure 3 shows Gaussian fits to the histograms of $\log(|J|)$. Table 2 reports the values of μ_{\log} and σ_{\log} determined both ways, and shows that, for all SAMs except SC₁₀ and SC₁₇, more than 80 % of the values of $\log(|J|)$ fall within the interval of $\mu_{\log} \pm \sigma_{\log}$ determined by the Gaussian fit. We will discuss the rationale and implications of the choice to fit Gaussians, rather than calculate the arithmetic mean and standard deviation, in detail in a separate paper.¹⁴¹

As noted above, we attribute the log normal distribution of J to a normal distribution of the distance between the top and bottom electrodes. According to the simplified Simmons relation (Equation 1), J is exponentially dependent on d . We hypothesize that the nature of defects on the SAM — a number of different *types* of defects, randomly distributed — lead to a normal distribution of d which, in turn, implies a normal distribution of $\log(|J|)$.

The SAM is At Least Partially Responsible for the Random Error in J . It is instructive to note the differences in σ_{\log} across the series of n-alkanethiols. According to Table 2, this parameter, in log-units, ranges from 0.45 – 1.6 when calculated as the arithmetic standard deviation of $\log(|J|)$, and from 0.29 – 1.1 when determined by fitting a Gaussian. No unambiguous trend in σ_{\log} vs. d emerges from the data, but σ_{\log} does appear to be smaller at the extremes of the series and larger in the middle (especially SC₁₄ and SC₁₅). Since the substrate and top-electrode remain invariant across the series of n-alkanethiols, we conclude that the large range in σ_{\log} is due to the SAM, and not the roughness of the Ag^{TS} electrode or variations in the morphology, composition, or

electrical properties of the Ga₂O₃/EGaIn electrode. We therefore believe that, despite the presence of incompletely defined components in our system, our measurements are sensitive to the properties of the SAM and useful for studying charge transport in organic matter.

Figure 3. Summary of current density, J , data derived from all n-alkanethiols.

Histograms of $\log|J|$ with a Gaussian fit include *all* the data collected by different users for n-alkanethiols (SC_n where $n = 9 - 18$); $N_{|J|}$ is the number of measurements collected for each SAM. A gradual decrease in the current density as chain length increases can be observed from the fitted data. The distributions tend to broaden as the number of data points increases due to slight user-to- user variations.

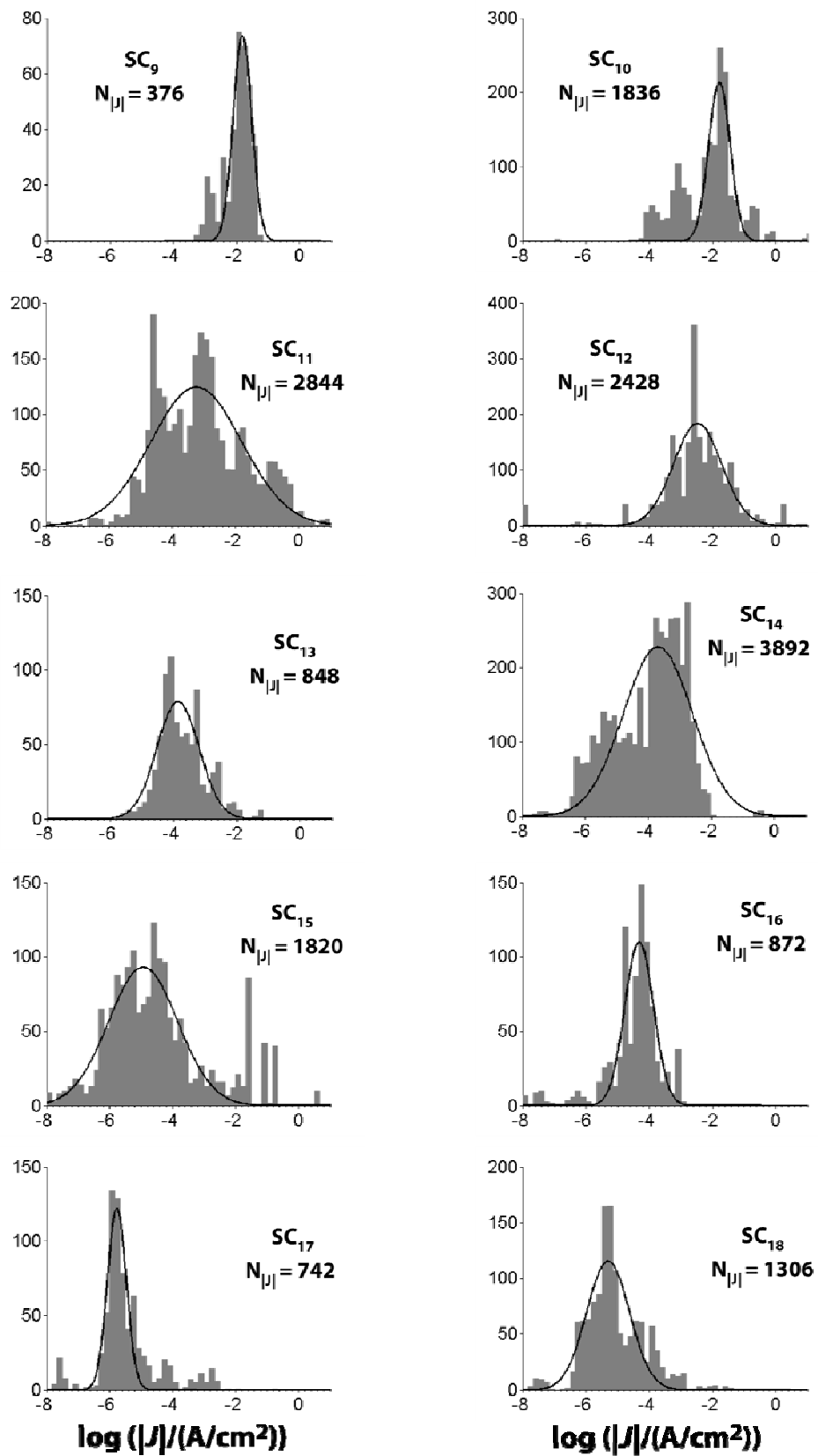


Fig 3:

Figure 4. A summary of data derived from the even numbered n-alkanethiols at different voltages (from a single user) to illustrate the consistency of the distribution of the data. We show two sets from positive bias and two from negative bias to illustrate that irrespective of the bias or the voltage ($|V| = 0.5$ or 0.25 V), the histograms look very similar. Similar observations were made with the odd series.

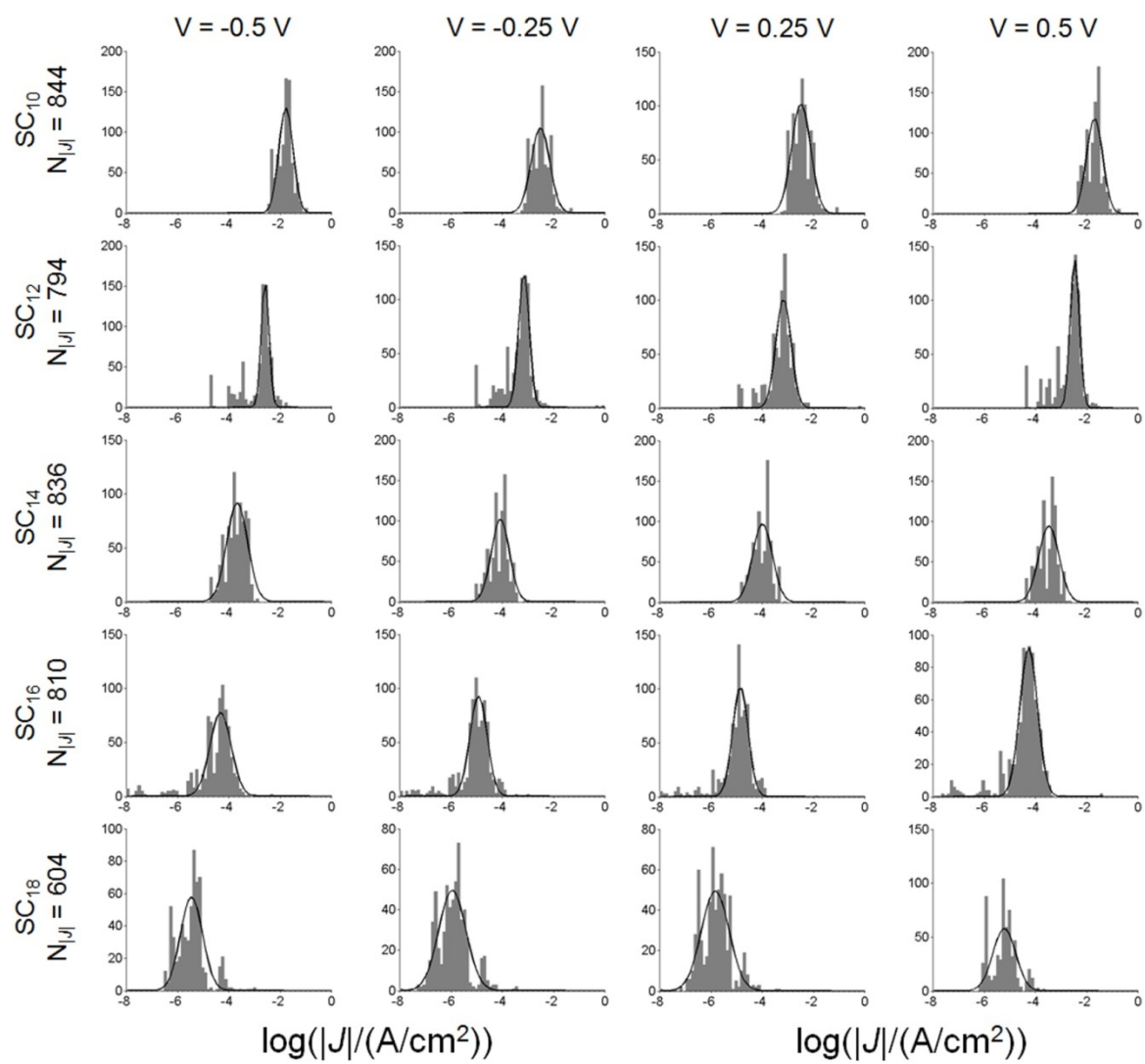


Fig. 4:

Figure 5. A plot of $\ln|\langle J \rangle|$ (V) at -0.5 V against the chain length of the n-alkanethiols, given in number of carbons, for all SAMs studied. Each point corresponds to the mean of the Gaussian fit to the histograms above (Figures 3) and the error bars represent the log-standard deviation. SAMs derived from even n-alkanethiols gave higher current densities than the analogous odd- series. For each series of n-alkanethiols — odd or even — the corresponding average J/V curves are given next to the plot of current densities at -0.5V.

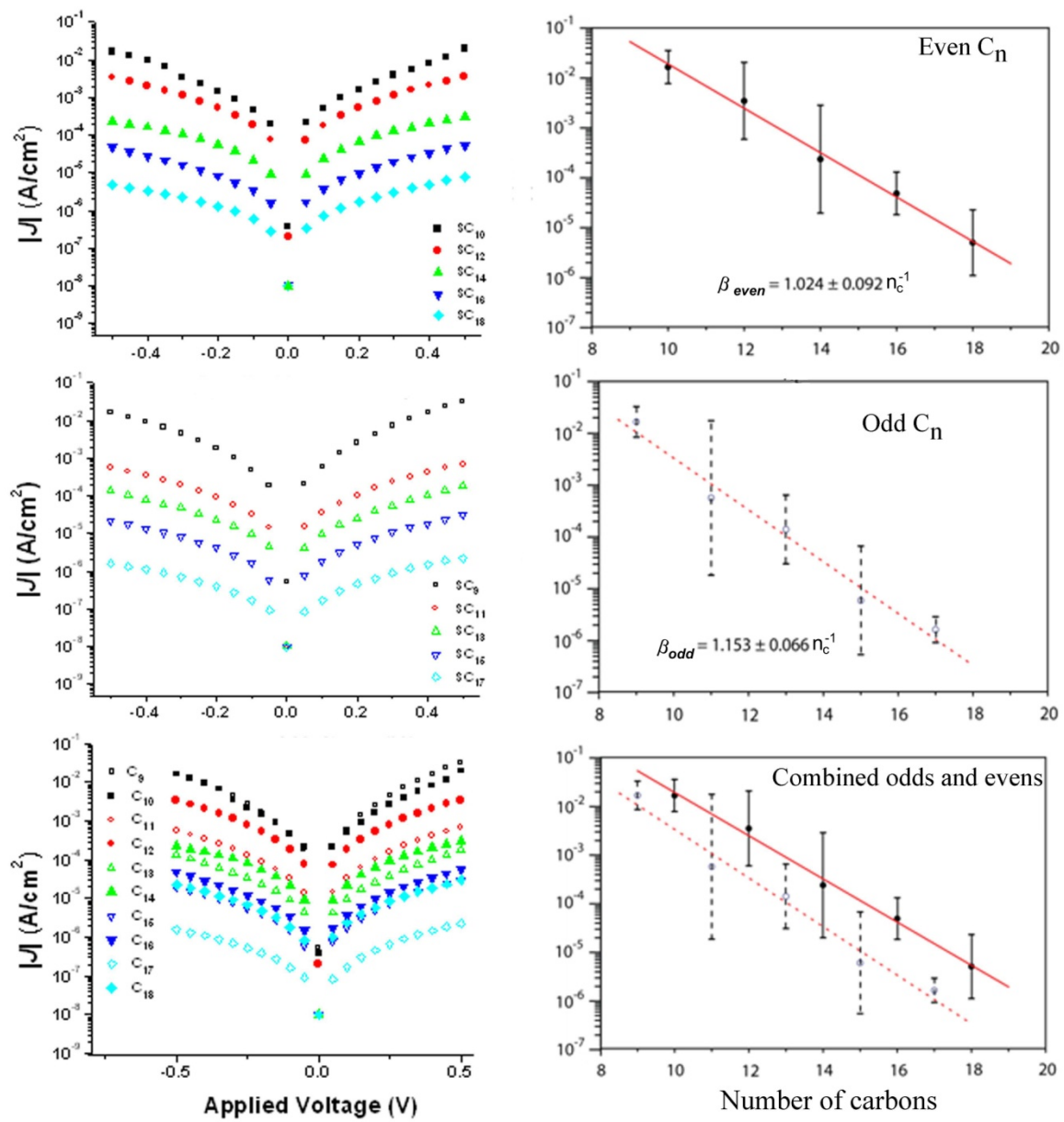


Fig. 5

Demonstrating the Odd-Even Effect. Figure 5 summarizes the results of fitting all the distributions of $\log(|J|)$ for *n*-alkanethiols. On the right column of Figure 5, we show the population mean of J , μ_J , (with error bars defined by σ_J) vs. chain length at $V = -0.5$ V for odd-numbered, even-numbered, and all alkanethiols, respectively. Similarly, on the left column of Figure 5, we show μ_J vs. applied bias (constituting an average $J(V)$ trace) for the same groupings of alkanethiols. For the odd- and even-numbered alkanethiols plotted separately, μ_J decreases exponentially with increasing chain length. In the combined dataset, however, the visible oscillation between increasing and decreasing μ_J suggests a measurable difference in charge transport between odd- and even-numbered *n*-alkanethiols.

The issue of whether or not there is such an “odd-even effect”, or just noise in a simple progression of J with chain length, revolves around the question of whether the odd-numbered and even-numbered alkanethiols are best regarded as two separate datasets requiring distinct analyses, or as one coherent dataset adequately described by parameters in common. Here, we give two simple, statistical justifications for regarding the odd-numbered and even-numbered alkanethiols as two separate datasets (we will discuss other, more complex reasons and statistical data in a separate paper).^{39,53,128,130}

i) When considered as separate datasets, both the odd and even alkanethiols exhibit an uninterrupted decrease in $\log(|J|)$ with increasing chain length, but when they are collected in a single dataset, this trend breaks down. Using a two-sample t-test, it is possible to compare two normally distributed samples to determine whether the samples come from populations with significantly different means, and to evaluate which of the means is greater. For example, comparing $\log(|J(-0.5V)|)$ between SC_{10} and SC_{12} using a

t-test leads to the conclusion, at the 99% confidence level, that $\mu_{\log,SC10} > \mu_{\log,SC12}$. It is important to note that the t-test assumes that the data being analyzed are normally distributed; thus, it is important to work with distributions of $\log(|J|)$, and not J , for this analysis. Applying the t-test separately to the two series of odd and even alkanethiols yields the following two sets of inequalities, valid at the 99% confidence level:

$$\mu_{\log,SC9} > \mu_{\log,SC11} > \mu_{\log,SC13} > \mu_{\log,SC15} > \mu_{\log,SC17} \quad (2)$$

and

$$\mu_{\log,SC10} > \mu_{\log,SC12} > \mu_{\log,SC14} > \mu_{\log,SC16} > \mu_{\log,SC18} \quad (3)$$

For both datasets, the trend of decreasing μ_{\log} with increasing chain length is statistically significant and unbroken. Applying the t-test to the combined dataset of odd and even alkanethiols, however, yields a different set of inequalities (see table 3):

$$\mu_{\log,SC9} > \mu_{\log,SC10} > \mu_{\log,SC11} < \mu_{\log,SC12} > \mu_{\log,SC13} > \mu_{\log,SC14} > \mu_{\log,SC15} \approx \mu_{\log,SC16} > \mu_{\log,SC17} < \mu_{\log,SC18} \quad (4)$$

The symbol “ \approx ” indicates that the t-test could not distinguish between the population means of $\log(|J(-0.5V)|)$ for SC_{15} and SC_{16} at the 99% confidence level. While the values of μ_{\log} generally decrease with increasing chain length, the reversal of the inequalities between SC_{11} and SC_{12} and between SC_{17} and SC_{18} is a clear deviation from the trend observed in the separate odd and even datasets and, thus, constitutes one piece of evidence for an odd-even effect.

ii) Linear regression of $\log(|J|)$ vs. chain length indicates that the odd and even alkanethiols belong to two separate datasets. As noted above, the rate of charge-transport through SAMs of alkanethiols decays exponentially with increasing chain-length, such that the relationship between $\log(|J|)$ and d is linear ($\log(|J|) = \log(|J_0|) - \log(e)\beta d$).

Linear least-squares fitting of $\log(|J|)$ vs. d gives estimates for the parameters J_0 and β , (discussed below) and determines the region that is 95% likely to contain the true fit (this region is bounded by so-called 95% confidence bands).¹⁴² We performed two separate linear fits of μ_{\log} vs. d , for odd and even alkanethiols, using the estimates of μ_{\log} at $V = -0.5$ V determined by fitting Gaussian functions to the histograms of $\log(|J(-0.5V)|)$, as described above.¹⁴³ Figure 6 shows these fits, along with their 95% confidence bands. A key feature of this plot is that the 95% confidence bands for the two fits do not overlap in the region between SC₁₁ and SC₁₈ (though they do overlap outside this region, see below). While we cannot claim, with statistical confidence, any difference in J_0 or β (see below) between the odd and even alkanethiols, we can state, with 95% confidence, that two separate lines fit the combined dataset of odd and even alkanethiols better than any single line. In other words, the odd and even alkanethiols are best regarded as distinct datasets, due to the presence of an odd-even effect resulting from an as-yet unidentified cause.

Separately fitting the data for odd- and even-numbered alkanethiols (data taken by several experimentalists, Figures 5a and 5b) to Equation 1 gives two values for the tunneling decay constant: $\beta_{\text{odd}} = 1.15 \pm 0.07 n_C^{-1}$ and $\beta_{\text{even}} = 1.02 \pm 0.09 n_C^{-1}$ at -0.5 V.

Figure 6. Plot of μ_{\log} vs. chain-length for odd (open blue circles) and even (closed black circles) alkanethiols. The solid lines are the best linear, least-squares fits to the odd (blue) and even (black) data. Dot-dashed blue lines represent the 95% confidence bands for the fit to the odd alkanethiols, and dashed black lines show the 95% confidence bands for the fit to the even alkanethiols. Error bars have been omitted for clarity. The two 95% confidence bands do not overlap in the region of SC₁₁ through SC₁₈, indicating that two different fits are warranted. The confidence bands do, however, overlap outside of this region, especially as the extrapolated fit approaches $n_C = 0$. Distinguishing between the slopes (related to β) and intercepts (related to J_0) of the two fits is, thus, difficult.

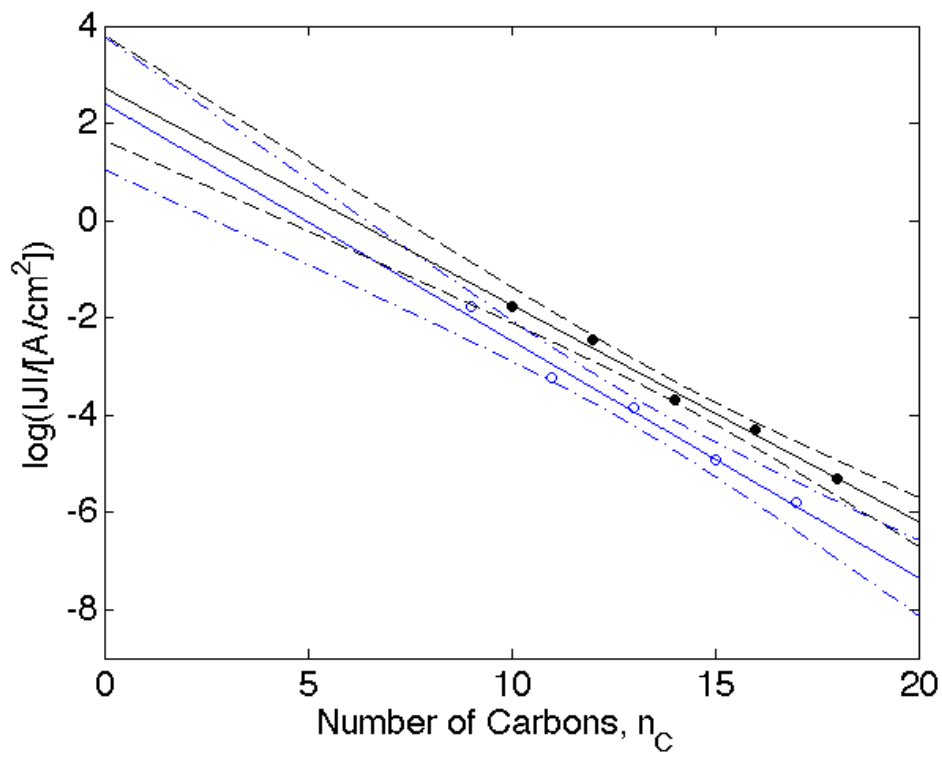


Figure 6.

The difference in these two values is not statistically significant, so we can conclude neither that they are the same nor that they differ. Comparing these data with data taken by a single user (Figure 7), we observe $\beta_{\text{odd}} = 1.19 \pm 0.08$ and $\beta_{\text{even}} = 1.05 \pm 0.06 n_C^{-1}$ at -0.5 V. Our value of β for the even n-alkanethiols occupies the high end of the range of values reported for systems using Hg-SAM electrodes and spin-cast polymer electrodes ($\beta_{\text{even}} = 0.71 - 1.1 n_C^{-1}$).^{66,67,78,144-147}

Likewise, the separate fits to Equation 1 of data from odd- and even-numbered alkanethiols give two log-normally distributed estimates for the pre-exponential factor: $\log(|J_{0,\text{odd}}|) = 2.42 \pm 0.68$ (i.e. $|J_{0,\text{odd}}| = 2.6 \times 10^2 \text{ A/cm}^2$ with a 95 % confidence interval of $1.1 \times 10 - 6.0 \times 10^3 \text{ A/cm}^2$) and $\log(|J_{0,\text{even}}|) = 2.73 \pm 0.54$ (i.e. $|J_{0,\text{even}}| = 5.4 \times 10^2 \text{ A/cm}^2$ with a 95 % confidence interval of $4.5 \times 10 - 6.5 \times 10^3 \text{ A/cm}^2$). Note that, in Figure 6, the 95 % confidence bands for the two linear fits do not overlap in the region containing the bulk of the data, but do substantially overlap when the fits are extrapolated to $n_C = 0$ in order to determine J_0 . Again, we emphasize that the magnitude of the error in these estimates makes it impossible to say, with statistical confidence, whether $J_{0,\text{odd}}$ and $J_{0,\text{even}}$ are the same or different. The lack of reported values of J_0 in the literature makes direct comparisons of this value across experimental platforms difficult.

Reproducibility. There are two axes along which to assess the reproducibility of measurements using $\text{Ag}^{\text{TS}}\text{-SC}_n//\text{Ga}_2\text{O}_3/\text{EGaIn}$ junctions: dependence on the technique of the operator, and dependence on the ambient conditions of measurement. Like any manual technique, the formation of conical tips of $\text{Ga}_2\text{O}_3/\text{EGaIn}$, and the formation of tunneling junctions using these tips, is an operator-dependent process.

Figure 7. A plot of $\ln|\langle J \rangle|$ (V) at -0.5 V against the chain length of the alkanethiols, given in number of carbons, for all SAMs as measured by a single user across either the odd- or even numbered n-alkanethiols. The observed values of β from single users are not significantly different from those obtained from measurements of a group of five users.

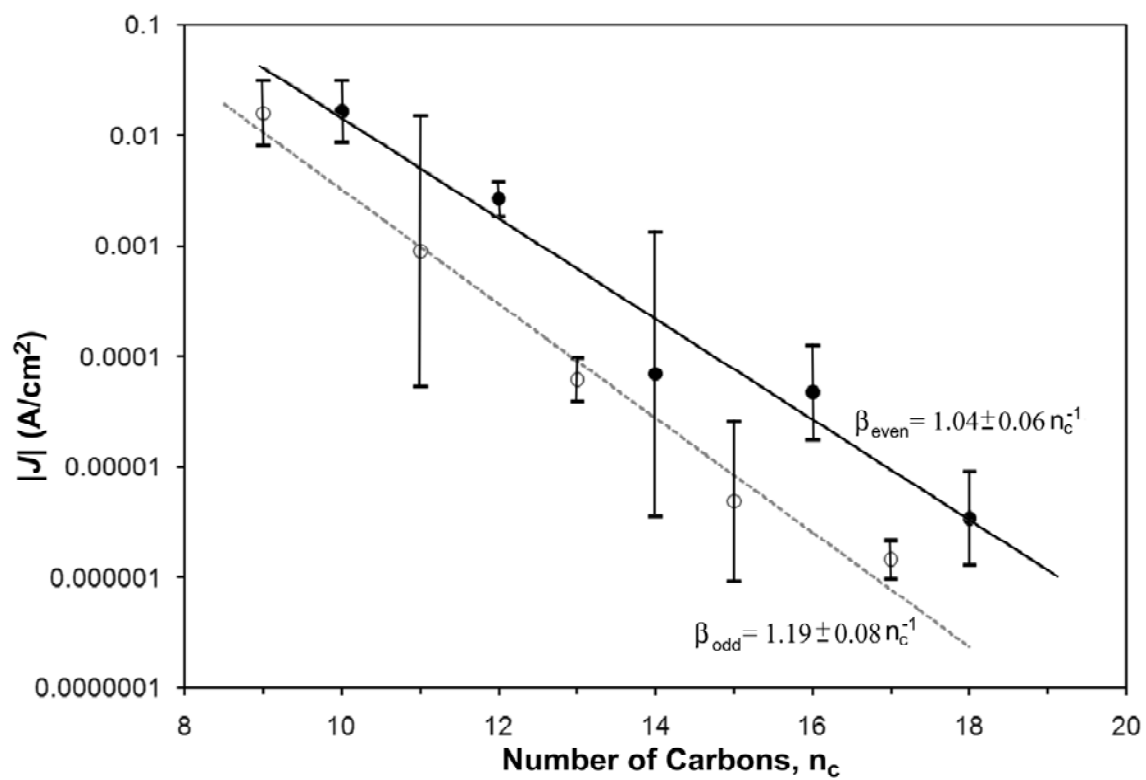


Fig. 7

Table 1. Yield and Other Parameters of Data Collected for Odd and Even Alkanethiols

<i>n</i>	users	samples	junctions	shorting junctions^a	N_J^b	non-shortening yield (%)^c
9	1	1	11	2	376	82
10	4	5	51	6	1836	88
11	4	10	105	13	2844	88
12	4	8	65	8	2428	88
13	2	3	21	1	848	95
14	4	12	101	4	3892	96
15	4	11	81	7	1820	91
16	2	2	21	0	872	100
17	4	5	27	4	742	85
18	3	5	45	1	1306	98

^a A short is defined in the text as a junction for which J exceeds 10^2 A/cm² at any time

^b The total number of values of J collected at each applied bias. No data were excluded.

^c Calculated as the ratio of non-shortening junctions to the total number of junctions.

Table 2. Comparison of Methods for Determining the Population Mean of $\log(|J|)$

n	$\mu_{\log} \pm \sigma_{\log}$ (calculated)^a	$\mu_{\log} \pm \sigma_{\log}$ (Gaussian fit)^b	Data within Gaussian (%)^c
9	-1.99 ± 0.45	-1.78 ± 0.29	87
10	-2.12 ± 1.0	-1.77 ± 0.32	60
11	-3.04 ± 1.4	-3.23 ± 0.44	94
12	-2.54 ± 1.3	-2.47 ± 0.77	89
13	-3.73 ± 0.74	-3.86 ± 0.66	95
14	-4.01 ± 1.1	-3.70 ± 1.1	99
15	-4.45 ± 1.6	-4.93 ± 1.1	88
16	-4.51 ± 0.90	-4.32 ± 0.45	92
17	-5.46 ± 0.98	-5.81 ± 0.23	73
18	-5.08 ± 0.93	-5.31 ± 0.66	93

^a Calculated by taking the arithmetic average and standard deviation of $\log(|J|)$ after excluding shorts.

^b The parameters of the Gaussian function that was the least-squares fit to the histogram of $\log(|J|)$. No data were excluded.

^c Defined as the percentage of values of $\log(|J|)$ that lie within three standard deviations above and below the mean (mean and standard deviation determined from the Gaussian fit)

Some parameters – notably, the speed with which an operator retracts the syringe to form the tip, the tolerance of the operator for deviations of the shape of the tip from the “ideal”, and the force with which an operator applies the tip to the SAM – are difficult to quantify and even more difficult to standardize across operators. Further, as we have noted above, the surface of the Ga₂O₃ is likely contaminated with a thin film of adsorbed organic material, and it is likely that the composition and thickness of this film depend on the local environment at the time of measurement. While we are currently pursuing strategies to minimize operator-dependence (through standardized formation of electrodes) and environmental dependence (by isolating the measurement stage in a chamber with a controlled atmosphere), the measurements described here are sufficiently reproducible to lend confidence to our conclusions.

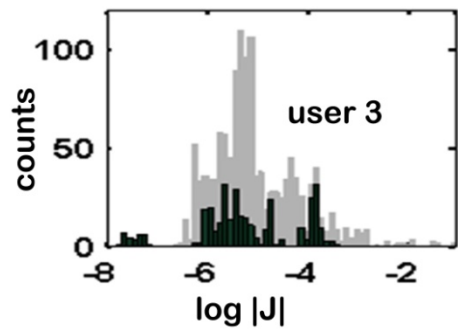
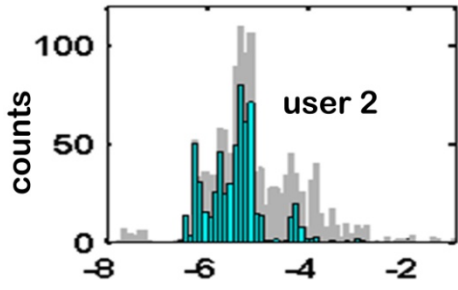
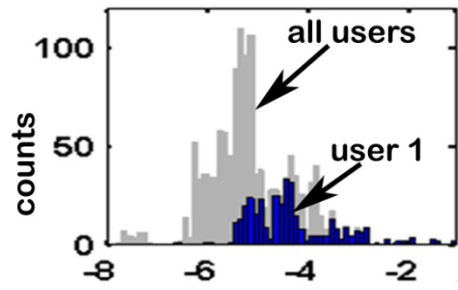
We point to two pieces of evidence to demonstrate the reproducibility of our results: the similarity of distributions of $\log(|J|)$ collected by multiple users for individual compounds, and the similarity of values of β calculated by a single user vs. multiple users.

Figure 8 shows the contributions of three different operators to the dataset of $\log(|J|)$ for SC₁₈ at $V = -0.5$ V (though it is typical of all compounds and all values of applied bias). These operators collected their data on different days under different ambient conditions. The histograms from individual users (color) are normal distributions of $\log(|J|)$ that collectively sum to the normal distribution of all values of $\log(|J|)$ (gray). The distribution from user 1 has $\mu_{\log} = -4.65 \pm 0.61$, that from user 2 has $\mu_{\log} = -5.44 \pm 0.41$, and that from user 3 has $\mu_{\log} = -5.24 \pm 0.97$, as determined from

fitting Gaussian functions to the histograms (see Table S2 in Supporting Information). While the means of these distributions are not identical, the error bars on these means do overlap substantially. Two-sample t-tests confirm that there is no statistically significant difference between the distributions from users 1 and 2 ($p = 0.16$), and from users 1 and 3 ($p = 0.16$). Interestingly, the test did find a statistically significant difference between users 2 and 3 ($p \ll 0.01$), but this may be due to the cluster of outliers, near $\log(|J|) = -4.0$, in the distribution of user 3. In any case, the variations between operators serve to broaden the overall distribution of $\log(|J|)$ for each compound, but does not preclude statistical comparisons across different compounds, as demonstrated above.

It is instructive to compare entire datasets, and not just single compounds, collected by a single user within a short timeframe (< 1 week) and by multiple users over a long timeframe (> 1 month). Figure 5 shows data for SC₉ through SC₁₈ collected by a total of six users, along with values for β_{even} and β_{odd} . By contrast, Figure 6 shows data for odd-numbered alkanethiols, collected by a single user, and for even-numbered alkanethiols, collected by a different individual (independently, both datasets derive from a single user). The error bars are generally smaller for the single-user datasets than for the datasets collected by multiple users; as noted above, however, the values of β determined for corresponding datasets are indistinguishable. Despite the evident challenges to reproducible formation of Ga₂O₃/EGaIn tips and measurement of tunneling junctions, therefore, we conclude that the reproducibility of these measurements is sufficient to draw conclusions with confidence from trends in the data.

Figure 8. Histograms of data collected for the octadecanethiol SAM from three different users. Data from a single analyst is shown with the pooled data from all users in the background (grey). These figures are representative of all compounds in both series (odd and even).



Conclusions

Measurements using $\text{Ag}^{\text{TS}}\text{-SC}_n\text{//Ga}_2\text{O}_3\text{/EGaIn}$ junctions demonstrated a difference in rates of charge transport through SAMs with odd-numbered and even-numbered n -alkanethiols. The sensitivity of this technique to the subtle differences in the structure of the SAM and its interface with the Ga_2O_3 layer arises from at least four factors: i) the use of ultra-flat metal surfaces (Ag^{TS}) to fabricate the SAMs, ii) the careful purification of the n -alkanethiols used to form SAMs, iii) the presence, on the $\text{Ga}_2\text{O}_3\text{/EGaIn}$ top-electrode, of a thin (~ 2 nm) layer of oxide that protected the junction from artifacts and shorts while not interfering with charge transport, and iv) the application of statistical analysis to a large number of measurements.

Though the $\text{Ga}_2\text{O}_3\text{/EGaIn}$ electrode has both advantages and disadvantages, it is demonstrably useful for physical-organic studies of charge transport.

$\text{Ag}^{\text{TS}}\text{-SAM//Ga}_2\text{O}_3\text{/EGaIn}$ junctions exhibit high yield ($> 80\%$) and, thus, allow for the collection of large amounts of data within a short time. These junctions do not require a cleanroom, an ultra-high vacuum, toxic substances such as Hg, a solvent bath, or a second SAM. They do, however, require a skilled user and attention to detail in order to yield meaningful results, primarily (we believe) because the formation of conical tips of $\text{Ga}_2\text{O}_3\text{/EGaIn}$ is a user-dependent process. We are working on determining and eliminating the elements of our procedure that contribute to this user-dependence, and thus standardizing the procedure.

The least well-defined component of this system is the thin (~ 2 nm) layer of Ga_2O_3 on the surface of the electrode, along with any organic material adsorbed on its surface. On one hand, this film of Ga_2O_3 , like protective layers in other techniques, helps

to prevent the formation of metal filaments; and so we believe that this layer is necessary to achieve high yields of working junctions. On the other hand, the morphology and electrical properties of the layer of Ga_2O_3 are not completely defined, and are possibly sensitive to how the electrode is formed. Based on the observation that the width of the distribution of J varies across the series of SAMs investigated, we conclude that the SAM contributes at least as significantly to the random error in our measurements as the layer of Ga_2O_3 .

While odd-even effects have been reported in studies of the properties of n -alkanethiols, the observation of an odd-even effect in the context of charge transport is important for three reasons: i) it provides a test for theoretical descriptions of charge transport through SAMs, ii) it demonstrates that the $\text{Ag}^{\text{TS}}\text{-SC}_n//\text{Ga}_2\text{O}_3/\text{EGaIn}$ junction measures properties of SAMs (as opposed to artifacts of the electrodes), and iii) it indicates the importance of the structure of near-contact interfaces in charge transport through SAMs.

While we were able to identify an odd-even effect with respect to J , the random error in our measurements was too large to reveal whether there was an odd-even effect in the tunneling decay constant, β , or the pre-exponential factor, J_0 . The odd-even effect must appear in one (or both) of these two parameters, because the effect must arise from a systematic odd-even variation of either i) the tunneling barrier posed by the SAM, or ii) the tunneling barrier at the interface between the SAM and the electrode. The current limitations of our statistical analysis prevent us from identifying the origin of this difference.

The measured values of the tunneling decay constant – $\beta_{\text{even}} = 1.15 \pm 0.07 \text{ nC}^{-1}$ for even-numbered alkanethiols and $\beta_{\text{odd}} = 1.02 \pm 0.09 \text{ nC}^{-1}$ for odd-numbered alkanethiols – both lie within, but at the high end of, the range of values reported in the literature (0.75 – 1.1 nC^{-1}). Again, we stress that the difference between the *measured* values of β_{even} and β_{odd} is not statistically significant.

Acknowledgements

This work was funded by NSF grant (grant CHE-05180055) to GMW, MT and JB were supported by Mary-Fieser postdoctoral fellowships and the NanoScience and Engineering Centre (NSEC) at Harvard University, the Netherlands Organization for Scientific Research (NWO) is kindly acknowledged for the Rubicon grant to C.A.N.

References

- (1) Dumke, M. F.; Tombrello, T. A.; Weller, R. A.; Housley, R. A.; Cirlin, E. H. *Surf. Sci.* **1983**, *124*, 407-422. And our unpublished results to be communicated elsewhere.
- (2) Tao, F.; Bernasek, S. L. *Chem. Rev.* **2007**, *107*, 1408-1453.
- (3) Love, J. C.; Estroff, L. A.; Kriebel, J. K.; Nuzzo, R. G.; Whitesides, G. M. *Chem. Rev.* **2005**, *105*, 1103-1169.
- (4) Nishi, N.; Hobara, D.; Yamamoto, M.; Kakiuchi, T. *J. Chem. Phys.* **2003**, *118*, 1904-1911.
- (5) Bai, B.; Wang, H.; Xin, H.; Long, B.; Li, M. *Liq. Cryst.* **2007**, *34*, 659-665.
- (6) Blumstein, A.; Blumstein, R. B. *Recent Adv. Liq. Cryst. Polym., [Proc. Eur. Sci. Found. Polym. Workshop Liq. Cryst. Polym. Syst.]*, 6th **1985**, 129-31.
- (7) Blumstein, A.; Thomas, O. *Macromolecules* **1982**, *15*, 1264-7.
- (8) Cacelli, I.; De Gaetani, L.; Prampolini, G.; Tani, A. *Mol. Cryst. Liq. Cryst.* **2007**, *465*, 175-186.
- (9) Capar, M. I.; Cebe, E. *Phys. Rev. E: Stat., Nonlinear, Soft Matter Phys.* **2006**, *73*, 061711/1-061711/8.
- (10) Capar, M. I.; Cebe, E. *J. Comput. Chem.* **2007**, *28*, 2140-2146.

- (11) Centore, R. *Liq. Cryst.* **2009**, *36*, 239-245.
- (12) Chang, H.-S.; Wu, T.-Y.; Chen, Y. *J. Appl. Polym. Sci.* **2002**, *83*, 1536-1546.
- (13) Cheng, S. Z. D.; Li, C. Y.; Jin, S.; Weng, X.; Zhang, D.; Bal, F.; Zhang, J. Z.; Harris, F. W.; Chien, L.-C.; Lotz, B. *PMSE Prepr.* **2003**, *89*, 88-89.
- (14) Dunn, C. J.; Le Masurier, P. J.; Luckhurst, G. R. *Phys. Chem. Chem. Phys.* **1999**, *1*, 3757-3764.
- (15) Haegele, C.; Wuckert, E.; Laschat, S.; Giesselmann, F. *ChemPhysChem* **2009**, *10*, 1291-1298.
- (16) Henderson, P. A.; Cook, A. G.; Imrie, C. T. *Liq. Cryst.* **2004**, *31*, 1427-1434.
- (17) Henderson, P. A.; Inkster, R. T.; Seddon, J. M.; Imrie, C. T. *J. Mater. Chem.* **2001**, *11*, 2722-2731.
- (18) Itahara, T.; Tamura, H. *Mol. Cryst. Liq. Cryst.* **2007**, *474*, 17-27.
- (19) Johannsmann, D.; Zhou, H.; Sonderkaer, P.; Wierenga, H.; Myrvold, B. O.; Shen, Y. R. *Phys. Rev. E: Stat. Phys., Plasmas, Fluids, Relat. Interdiscip. Top.* **1993**, *48*, 1889-96.
- (20) Kobayashi, K.; Yoshizawa, A. *Liq. Cryst.* **2007**, *34*, 1455-1462.
- (21) Kundu, B.; Pal, S. K.; Kumar, S.; Pratibha, R.; Madhusudana, N. V. *EuroPhysics Lett.* **2009**, *85*, 36002/1-36002/6.
- (22) Marcelis, A. T. M.; Koudijs, A.; Sudhoelter, E. J. R. *Thin Solid Films* **1996**, *284-285*, 308-312.
- (23) Noack, F. *Mol. Cryst. Liq. Cryst.* **1984**, *113*, 247-68.
- (24) Ojha, D. P.; Kumar, D.; Pisipati, V. G. K. M. *Cryst. Res. Technol.* **2002**, *37*, 881-889.
- (25) Ojha, D. P.; Kumar, D.; Pisipati, V. G. K. M. *Z. Naturforsch., A: Phys. Sci.* **2002**, *57*, 189-193.
- (26) Parri, O.; Coates, D.; Greenfield, S.; Goulding, M.; Verrall, M. *Mol. Cryst. Liq. Cryst. Sci. Technol., Sect. A* **1999**, *332*, 2783-2790.
- (27) Roviello, A.; Sirigu, A. *Makromol. Chem.* **1982**, *183*, 895-904.
- (28) Stals, P. J. M.; Smulders, M. M. J.; Martin-Rapun, R.; Palmans, A. R. A.; Meijer, E. W. *Chem.--Eur. J.* **2009**, *15*, 2071-2080.
- (29) Umadevi, S.; Jakli, A.; Sadashiva, B. K. *Soft Matter* **2006**, *2*, 875-885.
- (30) Umamaheswari, U.; Ajeetha, N.; Srinivas, G.; Ojha, D. P. *Bull. Pure Appl. Sci., Sec. D* **2008**, *27D*, 55-64.
- (31) Yamaguchi, A.; Watanabe, M.; Yoshizawa, A. *Liq. Cryst.* **2007**, *34*, 633-639.
- (32) Yoshizawa, A.; Chiba, S.; Ogasawara, F. *Liq. Cryst.* **2007**, *34*, 373-379.
- (33) Yung, K. L.; He, L.; Xu, Y.; Shen, Y. W. *J. Chem. Phys.* **2005**, *123*, 246101/1-246101/3.
- (34) Azzam, W.; Cyganik, P.; Witte, G.; Buck, M.; Woell, C. *Langmuir* **2003**, *19*, 8262-8270.
- (35) Kato, H. S.; Noh, J.; Hara, M.; Kawai, M. *J. Phys. Chem. B* **2002**, *106*, 9655-9658.
- (36) Kobayashi, T.; Seki, T. *Langmuir* **2003**, *19*, 9297-9304.

- (37) Shaporenko, A.; Brunnbauer, M.; Terfort, A.; Johansson, L. S. O.; Grunze, M.; Zharnikov, M. *Langmuir* **2005**, *21*, 4370-4375.
- (38) Wintgens, D.; Yablon, D. G.; Flynn, G. W. *J. Phys. Chem. B* **2003**, *107*, 173-179.
- (39) Stoliar, P.; Kshirsagar, R.; Massi, M.; Annibale, P.; Albonetti, C.; de Leeuw, D. M.; Biscarini, F. *J. Am. Chem. Soc.* **2007**, *129*, 6477-6484.
- (40) Auer, F.; Nelles, G.; Selligren, B. *Chem. Eur. J.* **2004**, *10*, 3232-3240.
- (41) Heimel, G.; Romaner, L.; Bredas, J.-L.; Zojer, E. *Langmuir* **2008**, *24*, 474-482.
- (42) Kikkawa, Y.; Koyama, E.; Tsuzuki, S.; Fujiwara, K.; Miyake, K.; Tokuhisa, H.; Kanamoto, M. *Chem. Commun.* **2007**, 1343-1345.
- (43) Lin, S.-Y.; Tsai, T.-K.; Lin, C.-M.; Chen, C.-h.; Chan, Y.-C.; Chen, H.-W. *Langmuir* **2002**, *18*, 5473-5478.
- (44) Cademartiri, L.; Mwangi, M. T.; Nijhuis, C. A.; Barber, J. R.; Sodhi, R. N. S.; Brodersen, P.; Kim, C.; Reus, W. F.; Whitesides George, M. **2010**, unpublished results.
- (45) Joachim, C. *New J. Chem.* **1991**, *15*, 223-9.
- (46) Manassen, Y.; Shachal, D. *Ann. N. Y. Acad. Sci.* **1998**, *852*, 277-289.
- (47) Shachal, D.; Manassen, Y. *Chem. Phys. Lett.* **1997**, *271*, 107-112.
- (48) Selzer, Y.; Salomon, A.; Cahen, D. *J. Phys. Chem. B* **2002**, *106*, 10432-10439.
- (49) Sun, Q.; Selloni, A.; Scoles, G. *ChemPhysChem* **2005**, *6*, 1906-1910.
- (50) Lindsay, S. M. *Jpn. J. Appl. Phys., Part 1* **2002**, *41*, 4867-4870.
- (51) Wang, W.; Lee, T.; Reed, M. A. *Phys. Rev. B: Condens. Matter Mater. Phys.* **2003**, *68*, 035416/1-035416/7.
- (52) Wang, W.; Lee, T.; Reed, M. A. *Nano Mol. Electron. Handb.* **2007**, 1/1-1/41.
- (53) Slowinski, K.; Chamberlain, R. V.; Miller, C. J.; Majda, M. *J. Am. Chem. Soc.* **1997**, *119*, 11910-11919.
- (54) Slowinski, K.; Fong, H. K. Y.; Majda, M. *J. Am. Chem. Soc.* **1999**, *121*, 7257-7261.
- (55) Kim, Y.-H.; Jang, S. S.; Goddard, W. A., III *J. Chem. Phys.* **2005**, *122*, 244703/1-244703/9.
- (56) Wang, G.; Yoo, H.; Na, S.-I.; Kim, T.-W.; Cho, B.; Kim, D.-Y.; Lee, T. *Thin Solid Films* **2009**, *518*, 824-828.
- (57) Song, H.; Kim, Y.; Ku, J.; Jang, Y. H.; Jeong, H.; Lee, T. *Appl. Phys. Lett.* **2009**, *94*, 103110/1-103110/3.
- (58) Wang, G.; Kim, T.-W.; Jang, Y. H.; Lee, T. *J. Phys. Chem. C* **2008**, *112*, 13010-13016.
- (59) Kim, T.-W.; Wang, G.; Lee, H.; Lee, T. *Nanotechnology* **2007**, *18*, 315204/1-315204/8.
- (60) Lee, T.; Wang, W.; Klemic, J. F.; Zhang, J. J.; Su, J.; Reed, M. A. *J. Phys. Chem. B* **2004**, *108*, 8742-8750.
- (61) Wang, W.; Lee, T.; Reed, M. A. *Physica E* **2003**, *19*, 117-125.
- (62) Akkerman, H. B.; Blom, P. W. M.; de Leeuw, D. M.; de Boer, B. *Nature* **2006**, *441*, 69-72.

- (63) Akkerman, H. B.; de Boer, B. *J. Phys.: Condens. Matter* **2008**, *20*, 013001/1-013001/20.
- (64) Akkerman, H. B.; Kronemeijer, A. J.; Harkema, J.; van Hal, P. A.; Smits, E. C. P.; de Leeuw, D. M.; Blom, P. W. M. *Org. Electron.* **2010**, *11*, 146-149.
- (65) Akkerman, H. B.; Kronemeijer, A. J.; van Hal, P. A.; de Leeuw, D. M.; Blom, P. W. M.; de Boer, B. *Small* **2008**, *4*, 100-104.
- (66) Akkerman, H. B.; Naber, R. C. G.; Jongbloed, B.; Van Halt, P. A.; Blom, P. W. M.; De Leeuw, D. M.; De Boer, B. *Proc. Natl. Acad. Sci.* **2007**, *104*, 11161-11166.
- (67) Akkerman Hylke, B.; Blom Paul, W. M.; de Leeuw Dago, M.; de Boer, B. *Nature* **2006**, *441*, 69-72.
- (68) Van Hal, P. A.; Smits, E. C. P.; Geuns, T. C. T.; Akkerman, H. B.; De Brito, B. C.; Perissinotto, S.; Lanzani, G.; Kronemeijer, A. J.; Geskin, V.; Cornil, J.; Blom, P. W. M.; De Boer, B.; De Leeuw, D. M. *Nat. Nanotechnol.* **2008**, *3*, 749-754.
- (69) Strong, L.; Whitesides, G. M. *Langmuir* **1988**, *4*, 546-58.
- (70) Ulman, A. *Chem. Rev.* **1996**, *96*, 1533-1554.
- (71) Chidsey, C. E. D.; Liu, G. Y.; Rowntree, P.; Scoles, G. *J. Chem. Phys.* **1989**, *91*, 4421-3.
- (72) Chidsey, C. E. D.; Loiacono, D. N. *Langmuir* **1990**, *6*, 682-91.
- (73) Outka, D. A.; Stohr, J.; Rabe, J. P.; Swalen, J. D.; Rotermund, H. H. *Phys. Rev. Lett.* **1987**, *59*, 1321-4.
- (74) Ulman, A.; Eilers, J. E.; Tillman, N. *Langmuir* **1989**, *5*, 1147-52.
- (75) Sellers, H.; Ulman, A.; Shnidman, Y.; Eilers, J. E. *J. Am. Chem. Soc.* **1993**, *115*, 9389-401.
- (76) Schlenoff, J. B.; Li, M.; Ly, H. *J. Am. Chem. Soc.* **1995**, *117*, 12528-36.
- (77) Weiss, E. A.; Kaufman, G. K.; Kriebel, J. K.; Li, Z.; Schalek, R.; Whitesides, G. M. *Langmuir* **2007**, *23*, 9686-9694.
- (78) Weiss, E. A.; Chiechi, R. C.; Kaufman, G. K.; Kriebel, J. K.; Li, Z.; Duati, M.; Rampi, M. A.; Whitesides, G. M. *J. Am. Chem. Soc.* **2007**, *129*, 4336-4349.
- (79) Song, H.; Lee, T.; Choi, N.-J.; Lee, H. *J. Vac. Sci. Technol., B: Microelectron. Nanometer Struct.--Process., Meas., Phenom.* **2008**, *26*, 904-908.
- (80) Song, H.; Lee, T.; Choi, N.-J.; Lee, H. *Appl. Phys. Lett.* **2007**, *91*, 253116/1-253116/3.
- (81) He, J.; Forzani, E. S.; Nagahara, L. A.; Tao, N.; Lindsay, S. *J. Phys.: Condens. Matter* **2008**, *20*, 374120/1-374120/8.
- (82) Cui, X. D.; Zarate, X.; Tomfohr, J.; Sankey, O. F.; Primak, A.; Moore, A. L.; Moore, T. A.; Gust, D.; Harris, G.; Lindsay, S. M. *Nanotechnology* **2002**, *13*, 5-14.
- (83) Cui, X. D.; Primak, A.; Zarate, X.; Tomfohr, J.; Sankey, O. F.; Moore, A. L.; Moore, T. A.; Gust, D.; Harris, G.; Lindsay, S. M. *Science* **2001**, *294*, 571-574.
- (84) Song, H.; Lee, H.; Lee, T. *Ultramicroscopy* **2008**, *108*, 1196-1199.
- (85) Yoo, H.; Choi, J.; Wang, G.; Kim, T.-W.; Noh, J.; Lee, T. *J. Nanosci. Nanotechnol.* **2009**, *9*, 7012-7015.
- (86) Kim, Y.; Song, H.; Kim, D.; Lee, T.; Jeong, H. *ACS Nano* **2010**, *4*, 4426-4430.
- (87) Venkataraman, B.; Breen, J. J.; Flynn, G. W. *At. Force Microsc./Scanning Tunneling Microsc., [Proc. U.S. Army Natick Res., Dev. Eng. Cent. Symp.]*, **1994**, 117-25.

- (88) Venkataraman, B.; Breen, J. J.; Flynn, G. W. *J. Phys. Chem.* **1995**, *99*, 6608-19.
- (89) Venkataraman, B.; Flynn, G. W.; Wilbur, J. L.; Folkers, J. P.; Whitesides, G. M. *J. Phys. Chem.* **1995**, *99*, 8684-9.
- (90) Bumm, L. A.; Arnold, J. J.; Cygan, M. T.; Dunbar, T. D.; Burgin, T. P.; Jones, L., II; Allara, D. L.; Tour, J. M.; Weiss, P. S. *Science* **1996**, *271*, 1705-07.
- (91) Reed, M. A.; Zhou, C.; Muller, C. J.; Burgin, T. P.; Tour, J. M. *Science* **1997**, *278*, 252-254.
- (92) Chen, J.; Reed, M. A. *Chem. Phys.* **2002**, *281*, 127-145.
- (93) Lee, T.; Wang, W.; Reed, M. A. *Jpn. J. Appl. Phys., Part 1* **2005**, *44*, 523-529.
- (94) Wang, W.; Lee, T.; Reed, M. A. *J. Phys. Chem. B* **2004**, *108*, 18398-18407.
- (95) Kushmerick, J. G.; Holt, D. B.; Pollack, S. K.; Ratner, M. A.; Yang, J. C.; Schull, T. L.; Naciri, J.; Moore, M. H.; Shashidhar, R. *J. Am. Chem. Soc.* **2002**, *124*, 10654-10655.
- (96) Kushmerick, J. G.; Holt, D. B.; Yang, J. C.; Naciri, J.; Moore, M. H.; Shashidhar, R. *Phys. Rev. Lett.* **2002**, *89*, 086802.
- (97) Kushmerick, J. G.; Naciri, J.; Yang, J. C.; Shashidhar, R. *Nano Lett.* **2003**, *3*, 897-900.
- (98) Ashwell, G. J.; Mohib, A.; Miller, J. R. *J. Mater. Chem.* **2005**, *15*, 1160-1166.
- (99) Tran, E.; Rampi, M. A.; Whitesides, G. M. *Angew. Chem., Int. Ed.* **2004**, *43*, 3835-3839.
- (100) York, R. L.; Slowinski, K. *J. Electroanal. Chem.* **2003**, *550-551*, 327-336.
- (101) Chabinyk, M. L.; Holmlin, R. E.; Haag, R.; Chen, X.; Ismagilov, R. F.; Rampi, M. A.; Whitesides, G. M. *ACS Symp. Ser.* **2003**, *844*, 16-35.
- (102) Anariba, F.; McCreery, R. L. *J. Phys. Chem. B* **2002**, *106*, 10355-10362.
- (103) Slowinski, K.; Majda, M. *J. Electroanal. Chem.* **2000**, *491*, 139-147.
- (104) Slowinski, K.; Chamberlain, R. V., II; Bilewicz, R.; Majda, M. *J. Am. Chem. Soc.* **1996**, *118*, 4709-10.
- (105) Mann, B.; Kuhn, H. *J. Appl. Phys.* **1971**, *42*, 4398-405.
- (106) Akkerman, H. B.; Kronemeijer, A. J.; Blom, P. W. M.; van Hal, P.; de Leeuw, D. M.; de Boer, B. *Mater. Res. Soc. Symp. Proc.* **2008**, *1091E*, Paper #: 1091-AA02-05.
- (107) Bain, C. D.; Whitesides, G. M. *Angew. Chem., Int. Ed.* **1989**, *101*, 522-8.
- (108) Guo, Q.; Sun, X.; Palmer, R. E. *Phys. Rev. B: Condens. Matter Mater. Phys.* **2005**, *71*, 035406/1-035406/5.
- (109) Heimel, G.; Romaner, L.; Zojer, E.; Bredas, J.-L. *Proc. SPIE* **2008**, *6999*, 699919/1-699919/12.
- (110) Hostetler, M. J.; Murray, R. W. *Curr. Opin. Colloid Interface Sci.* **1997**, *2*, 42-50.
- (111) Kumar, A.; Abbott, N. L.; Biebuyck, H. A.; Kim, E.; Whitesides, G. M. *Acc. Chem. Res.* **1995**, *28*, 219-26.
- (112) Romaner, L.; Heimel, G.; Zojer, E. *Phys. Rev. B: Condens. Matter Mater. Phys.* **2008**, *77*, 045113/1-045113/9.

- (113) Schreiber, F. *J. Phys.: Condens. Matter* **2004**, *16*, R881-R900.
- (114) Ulman, A. *Thin Solid Films* **1996**, *273*, 48-53.
- (115) Ulman, A. *Mol. Solid State* **1999**, *2*, 1-38.
- (116) Ulman, A. *Acc. Chem. Res.* **2001**, *34*, 855-863.
- (117) Ulman, A.; Evans, S. D.; Shnidman, Y.; Sharma, R.; Eilers, J. E. *Adv. Colloid Interface Sci.* **1992**, *39*, 175-224.
- (118) Ulman, A.; Kang, J. F.; Shnidman, Y.; Liao, S.; Jordan, R.; Choi, G.-Y.; Zaccaro, J.; Myerson, A. S.; Rafailovich, M.; Sokolov, J.; Fleischer, C. *Rev. Mol. Biotechnol.* **2000**, *74*, 175-188.
- (119) Wang, W.; Lee, T.; Kretzschmar, I.; Routenberg, D.; Reed, M. A. *Tech. Dig. - Int. Electron Devices Meet.* **2004**, 531-532.
- (120) Wang, W.; Lee, T.; Reed, M. A. *Rep. Prog. Phys.* **2005**, *68*, 523-544.
- (121) Wang, W.; Lee, T.; Reed, M. A. *Proc. IEEE* **2005**, *93*, 1815-1824.
- (122) Wang, W.; Lee, T.; Reed, M. A. *Nanoscale Assem.* **2005**, 43-64.
- (123) Wang, W.; Lee, T.; Reed, M. A. *Lect. Notes Phys.* **2005**, *680*, 275-300.
- (124) Whitesides G., M.; Kriebel, J. K.; Love, J. C. *Sci. Prog.* **2005**, *88*, 17-48.
- (125) Whitesides, G. M.; Ferguson, G. S.; Allara, D.; Scherson, D.; Speaker, L.; Ulman, A. *Crit. Rev. Surf. Chem.* **1993**, *3*, 49-65.
- (126) Whitesides, G. M.; Gorman, C. B. In *The Handbook of Surface Imaging and Visualization*; Hubbard, A. T., Ed.; CRC press inc: Boca Raton, 1995, p 713-32.
- (127) Whitesides, G. M.; Laibinis, P. E. *Langmuir* **1990**, *6*, 87-96.
- (128) Salomon, A.; Cahen, D.; Lindsay, S.; Tomfohr, J.; Engelkes, V. B.; Frisbie, C. D. *Adv. Mater.* **2003**, *15*, 1881-1890.
- (129) Milani, F.; Grave, C.; Ferri, V.; Samori, P.; Rampi, M. A. *ChemPhysChem* **2007**, *8*, 515-518.
- (130) Akkerman, H. B. PhD Thesis, University of Groningen, 2008.
- (131) Ulman, A. *MRS Bull.* **1995**, *20*, 46-51.
- (132) Nijhuis, C. A.; Reus, W. F.; Whitesides, G. M. *J. Am. Chem. Soc.* **2009**, *131*, 17814-17827.
- (133) Chiechi, R. C.; Weiss, E. A.; Dickey, M. D.; Whitesides, G. M. *Angew. Chem., Int. Ed.* **2008**, *47*, 142-144.
- (134) Nijhuis, C. A.; Reus, W. F.; Barber, J. R.; Dickey, M. D.; Whitesides, G. M. *Nano Lett.* **2010**, *10*, 3611-3619.
- (135) Dickey, M. D.; Chiechi, R. C.; Larsen, R. J.; Weiss, E. A.; Weitz, D. A.; Whitesides George, M. *Adv. Funct. Mater.* **2008**, *18*, 1097-1104.
- (136) Song, H.; Kim, Y.; Jeong, H.; Reed, M. A.; Lee, T. *J. Phys. Chem. C* **2010**, ASAP.
- (137) Wang, W.; Lee, T.; Kretzschmar, I.; Reed, M. A. *Nano Lett.* **2004**, *4*, 643-646.
- (138) Song, H.; Lee, H.; Lee, T. *J. Am. Chem. Soc.* **2007**, *129*, 3806-3807.
- (139) Wang, G.; Kim, T.-W.; Jo, G.; Lee, T. *J. Am. Chem. Soc.* **2009**, *131*, 5980-5985.
- (140) Wold, D. J.; Frisbie, C. D. *J. Am. Chem. Soc.* **2000**, *122*, 2970-2971.
- (141) Reus, W. F.; Mwangi, M. T.; Barber, J. R.; Whitesides George, M.; Harvard University: **2010**, unpublished results.

(142) Not to be confused with 95% prediction bands, which define the region in which the results of the next measurement is likely to appear.

(143) It is also possible to perform linear regressions directly on $\log(|J|)$ vs. d without determining $\mu\log$ first. This direct approach offers distinct advantages but requires a more detailed analysis than we can present here; we will discuss this approach in a separate paper

(144) Holmlin, R. E.; Haag, R.; Chabinye, M. L.; Ismagilov, R. F.; Cohen, A. E.; Terfort, A.; Rampi, M. A.; Whitesides, G. M. *J. Am. Chem. Soc.* **2001**, *123*, 5075-5085.

(145) Holmlin, R. E.; Ismagilov, R. F.; Haag, R.; Mujica, V.; Ratner, M. A.; Rampi, M. A.; Whitesides, G. M. *Angew. Chem., Int. Ed.* **2001**, *40*, 2316-2320.

(146) Rampi, M. A.; Schueller, O. J. A.; Whitesides, G. M. *Appl. Phys. Lett.* **1998**, *72*, 1781-1783.

(147) Rampi, M. A.; Whitesides, G. M. *Chem. Phys.* **2002**, *281*, 373-391.